ELSEVIER

Journal of Power Sources 102 (2001) 233–241

JOURNAL OF POWER SOURCES

www.elsevier.com/locate/jpowsour

Cyclic voltammetric behavior of the lead electrode in sodium sulfate solutions

E.E. Abd El Aal*

Chemistry Department, Faculty of Science, Zagazig University, Zagazig, Egypt

Abstract

Cyclic voltammograms (CVs) of the Pb electrode were obtained in Na_2SO_4 solutions as a function of starting potential, electrolyte concentration, voltage range and voltage scanning rate. The shape of the voltammograms was found to depend on the starting potential as well on the sweep number. This is probably due to changes in the activation state of the electrode surface. In the first sweep, the anodic portion of the voltammograms is characterized by a shoulder and three peaks as a result of the formation of $PbSO_4$, PbO, PbO_2 and transformation of $PbSO_4$ to PbO_2, respectively, on the electrode surface before the evolution of oxygen. On the other hand, in the second and later sweeps, an additional anodic peak appeared which may be due to the formation of intermediate oxides. The cathodic portion shows the occurrence of three peaks corresponding to the reduction of PbO_2 to $PbSO_4$, PbO_2 to PbO and the latter with $PbSO_4$ to spongy lead, respectively, followed by the formation of PbH_2 before evolution of hydrogen. A correlation was made between the anodic peaks and their corresponding cathodic ones. Increasing the sulfate anion concentration increased the highest of the peak currents and shifted the anodic peak potentials towards more negative values. A linear relationship was obtained between the logarithm of the anodic peak current densities and the logarithm of SO_4^{2-} anion concentration. An increase in the scan rate enhanced the current density of both the anodic and cathodic branches. Also, the anodic potentials are shifted towards more positive values, whereas the cathodic peaks are shifted in the negative direction, indicating irreversible formation of the passive film on the electrode surface.

Keywords: Cyclic voltammograms; Lead; Behavior; Sodium sulfate; Passivation and lead oxides

1. Introduction

The electrochemical behavior of the Pb electrode is of great importance owing to its use in lead-acid batteries. There are many studies on its electrochemical behavior in various acid and alkaline solutions, mainly in order to understand its mechanism of operation during charging and discharging in lead-acid batteries [1–3]. Also, lead has a variety of applications in industry, particularly as a lining and piping material because of its good corrosion resistance in acidic media [4] and as a storage material for nuclear waste in deep underground vaults in the future [5]. Since the sulfate anion is in countered in several of these applications, it is important to study the electrochemical behavior of lead in sulfate solutions.

Early researches [6–9] concerning the anodic behavior of lead in sulfate solutions, carried out under galvanostatic and potentiostatic techniques, have indicated that a $PbSO_4$ layer forms initially. On increasing the potential further in the positive direction, an inner layer of PbO builds up progressively beneath the $PbSO_4$ porous layer. As potentials are set more positive PbO_2 becomes the predominant anodic surface product. Recent work carried out under galvanostatic condition by Abd El Aal [10], found that at relatively low current densities, a soluble Pb^{2+} and/or $HPbO^{2-}$ species was formed through the pores of the lead sulfate layer. The anodic polarization curves did not reach the potential for oxygen evolution. At higher current densities, the anodic polarization curve was characterized by four distinct arrests corresponding to the formation of $PbSO_4$, PbO, PbO_n and PbO_2, respectively, followed by transformation of $PbSO_4$ to PbO_2 on the electrode surface before the evolution of oxygen.

The present paper is concerned with the study of the electrochemical behavior of lead in Na_2SO_4 solution employing the cyclic voltammetric technique. The influence of starting potential, sulfate concentration, scanning range and scanning rate were examined. Some interesting features concerning both the corrosion and passivation processes are disclosed.

2. Experimental

Spectroscopically pure Pb (Johnson–Matthey, UK) was used as the test material in the form of short rods, 0.92 cm in diameter. The electrode was fixed to borosilicate glass tube

* Fax: +20-55-2303252.

0378-7753/01/$ – see front matter
PII: S0378-7753(01)00804-7

with epoxy resin so that the total exposed surface area was 0.69 cm^2. Electrical contact was achieved through a copper wire soldered to the end of the Pb rod but not exposed to the solution. Before being used, the electrode surface was polished with 0-, 00- and 000-grade emery papers, until it appeared free of scratches and other defects. Then, it was rinsed with acetone and finally with triply-distilled water.

The cell used for CV measurements was composed of two compartments separated by a sintered glass disc (grade G-3) to prevent mixing of the anodic and cathodic reaction products. The cell has a double wall jacket through which, water at the adjusted temperature was circulated. A conventional three-electrode system was used. A platinum sheet was used as auxiliary electrode, the working electrode was a lead, the reference electrode was saturated calomel electrode (SCE) with a luggin capillary positioned close to the working electrode surface in order to minimize Ohmic potential drop.

The potential of the working electrode was controlled by a Wenking Potentioscan type POS 73. The CVs were recorded on an *X–Y* recorder (Advance AR-2000). The CVs may be repeated three times without withdrawing the electrode from the electrolyte to examine the influence of the number of repeated cycles on the characteristics of the CVs.

The electrolytic solutions were prepared from analytical grade reagents and triply-distilled water. Experiments were carried out at a constant temperature $25 \pm 0.1^{\circ}C$. The cell temperature was controlled using ultra thermostat type Polyscience (USA). Each run was carried out in a fresh test solution and with a newly polished electrode.

3. Results and discussion

3.1. Effect of starting potential

Fig. 1 shows the curves of three different CVs starting from the quasi-steady-state potential ($E = -0.650$ V versus SCE), in 0.1 M Na_2SO_4 solution at a sweep rate 35 mV s^{-1}. The first curve represents the first sweep, the second and third sweeps are also illustrated. Comparison after forward and backward sweeps shows that the processes involved are irreversible. Also, the fact that the curves of the three successive sweeps are different indicates a change in the initial state of the Pb electrode. After the first sweep, the electrode surface is thought to be covered partially by the oxidation products that have not been reduced. Therefore, the second and third sweeps are quite different, as would be expected. The initial state of the electrode determines, to a large extent, the shape of the resulting CVs, as can be seen by inspection of the curves of Figs. 2–4. In these figures, the electrode was polarized cathodically at −1250, −2000 and −2400 mV, respectively, for 10 min before starting the CVs. In all cases, the behavior demonstrated by the CVs is quite different from that in Fig. 1. Similar observation was found previously during the study of the behavior of Pb in Na_2CO_3 solutions [11].

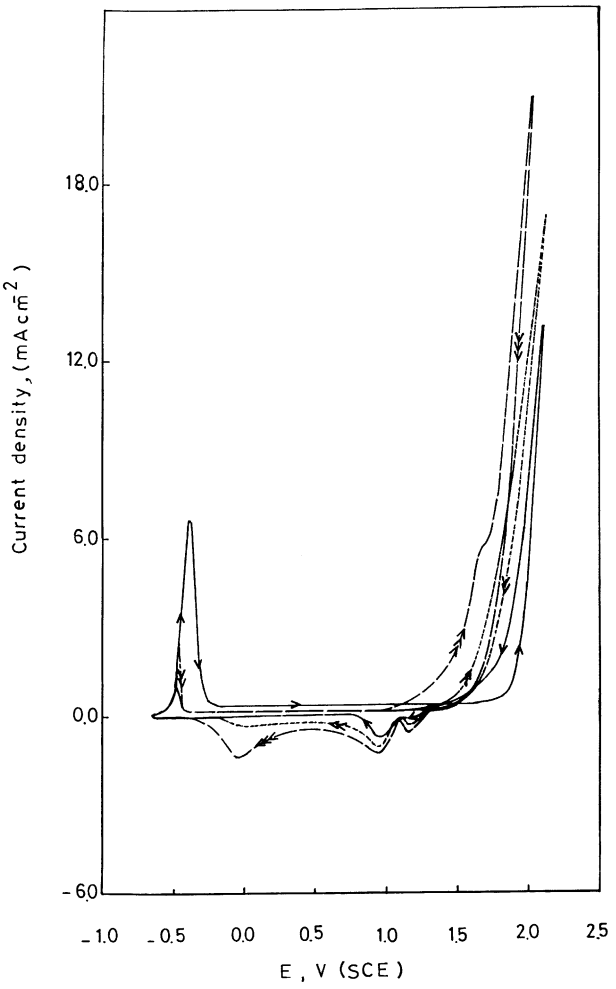

Fig. 1. Scanning voltammograms of the lead electrode in 0.1 M Na_2SO_4 solution starting from open-circuit potential, −0.650 V vs. SCE, at scanning rate of 35 mV s^{-1}. Sweep: (—) 1, (- - -) 2, (– – –) 3.

From the results in Figs. 1–4, one can conclude that the initial state of the electrode surface seems to be an important factor affecting the form of the current density–potential curves. Thus, if polarization was started from −0.650 V, the electrode surface would be covered with a pre-immersion oxide film, which may arise from the oxidation of the metal surface in the atmosphere or from the corrosion reactions taking place at the open-circuit potential [11–13]. Undoubtedly, the resulting CVs will be a function of these different starting conditions. However, at a starting potential of −2.4 V versus SCE (Fig. 4), hydrogen evolution takes place. In this case, the oxide film on the electrode surface can totally be reduced and a reproducible initial state of the electrode surface is achieved. These starting conditions are of importance for the comparison of these different results [11–14].

In Fig. 4, the CVs reported between −2.4 and +2.2 V versus SCE exhibit several regions that change during the reported cycles. In the first anodic half-cycle, three peaks (A_1, A_3, A_4) and a shoulder A_1^-, have been observed. Peak

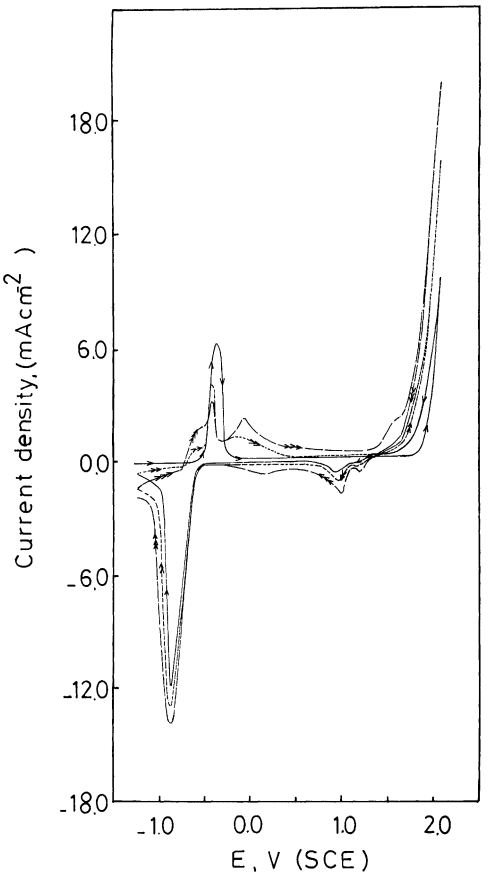

Fig. 2. Scanning voltammograms of the lead electrode in 0.1 M Na_2SO_4 solution, prepolarized for 10 min at −1.250 V vs. SCE, at scanning rate of 35 mV s^{-1}. For key, see Fig. 1.

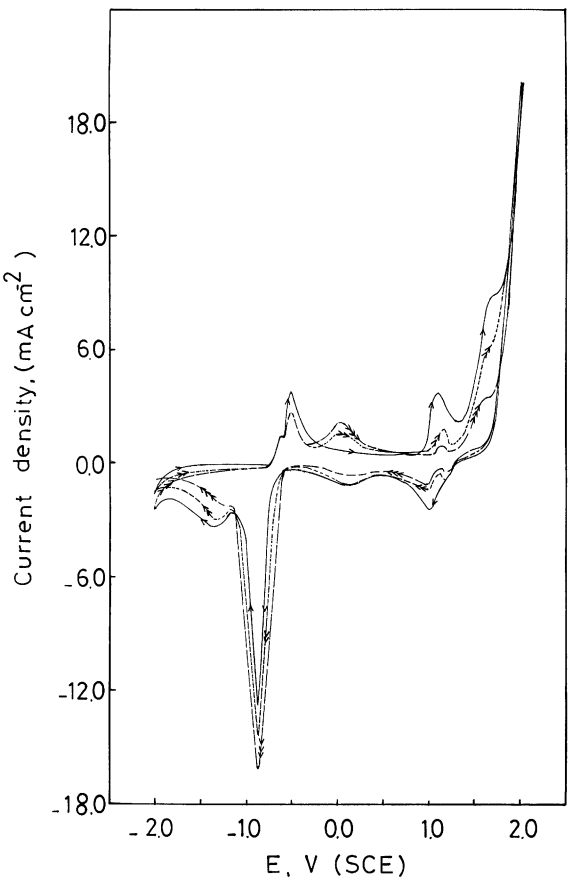

Fig. 3. Scanning voltammograms of the lead electrode in 0.1 M Na_2SO_4 solution, prepolarized for 10 min at −2.000 V vs. SCE, at scanning rate of 35 mV s^{-1}. For key, see Fig. 1.

A_1 is recorded at −0.540 V, which is preceded by shoulder A_1^- at −0.650 V. Also, the stable passive region, A_2, is observed to extend to about +0.875 V. Peak A_3 is recorded at about 1.025 V. The final anodic peak A_4 is found to start at around +1.325 V. In the vicinity of +1.750 V, the contribution of the oxygen evolution current is also manifested. During the cathodic half-cycle, peaks C_1, C_2, C_3 and C_4 appear at about +1.000, +0.125, −0.950 and −2.275 V, respectively. It is noted that, in the subsequent anodic sweeps (2 and 3), peak A_2^- appears at +0.025 V in the passive region while peak A_4 merges into the oxygen evolution current. These changes may be due to the difference in the initial state of the electrode surface. Also, it is of interest to observe a gradual shift in the anodic peak potentials with repeated cycling towards less negative values and a shift in the cathodic peak potentials to more negative values. Such behavior is attributed to both the slightly high scan rate used and irreversibility of the reactions.

Correlation between the observed peaks and the electrode reactions taking place can be achieved. The CVs of the lead electrode in Na_2SO_4 solutions exhibit a complex feature. The data in Fig. 4, reveal that the first anodic portion of the CVs has the same general characteristics as those reported in galvanostatic and potentiostatic measurements for Pb in Na_2SO_4 solutions [6–10]. As the potential moves in the positive direction, the current density decreases until it reaches a zero value at a definite potential value. At this point, the rate of the cathodic reaction: $2H^+ + 2e = H_2$, is equal to that of the anodic process: $Pb = Pb^{2+} + 2e$. When the electrode potential moves more positive, the anodic process is favored while the hydrogen evolution reaction is hindered and soon ceases [15–18]. Under these conditions, the anodic current density is equivalent to the dissolution rate of Pb. The current density increases steadily with the potential to give a shoulder A_1^-. This shoulder corresponds to the formation of a thin $PbSO_4$ layer on the electrode surface according to [6–10]

$$Pb + {SO_4}^{2-} = PbSO_4 + 2e \quad (1)$$

The shoulder A_1^- is followed by a sharp current rise leading to the first major anodic peak, A_1. The peak potential recorded at −0.540 V nearly coincides with the calculated [19] value for the Pb/PbO potential. Hence, the peak A_1 can be assigned to the electroformation of $Pb(OH)_2$ and/or PbO. This may be takes place through the highly ion-selective $PbSO_4$ layer, which is non-permeable for ${SO_4}^{2-}$ or Pb^{2+}

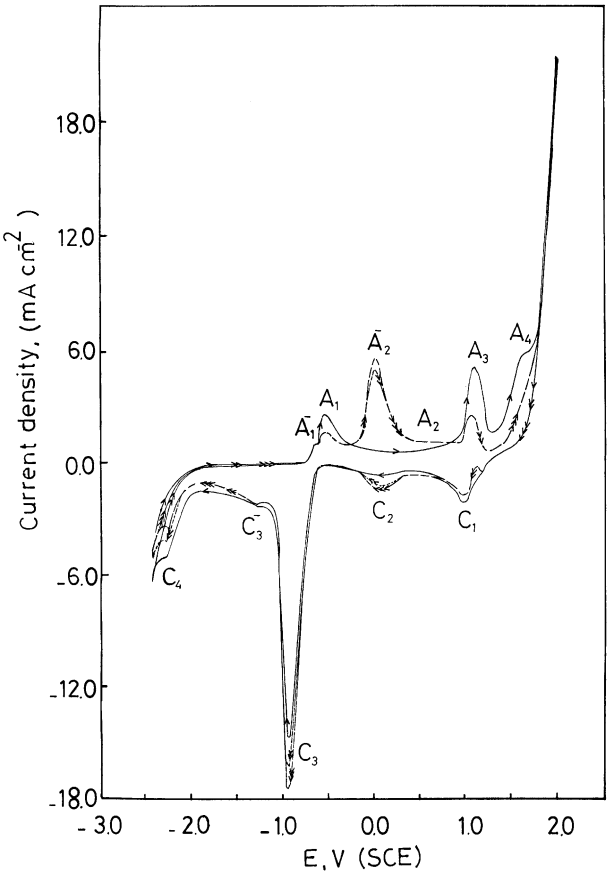

Fig. 4. Scanning voltammograms of the lead electrode in 0.1 M Na_2SO_4 solution, prepolarized for 10 min at −2.400 V vs. SCE, at scanning rate of 35 mV s^{-1}. For key, see Fig. 1.

ions, but permeable for H^+ and OH^- [20,21]. Thus, the lead ions generated at the lead surface during the anodization will react with the OH^- ions, diffusing through the pores of the $PbSO_4$ layer to produce PbO, according to the following reactions [6–11,14,22]:

$$Pb + OH^- = (PbOH)_{ads} + e \quad (2)$$

$$(PbOH)_{ads} + OH^- = Pb(OH)_2 + e \quad (3)$$

$$Pb(OH)_2 = PbO + H_2O \quad (4)$$

After peak A_1, the electrode becomes passive and the current density decreases to lower values (region A_2) and extends over a wide potential range. The passive current density increases quite slowly as the potential shifts to more positive values. This increase may plausibly be due to the establishment of a new process on the electrode surface that is likely to be the transformation of PbO to PbO_2 [10,11,23] at peak A_3 (the second major anodic peak). It is of interest to note that, in the subsequent sweeps 2 and 3, the passive region (A_2) appear as a peak A_2^- which possibly corresponds to the formation of intermediate oxides such as Pb_2O_3, Pb_3O_4 or PbO_n (where $1 \leq n \leq 2$) [14]. Such behavior may be attributed to the fact that the products, which formed during the anodic half-cycle, are reduced during the cathodic half-cycle. Thus, it could be expected that the surface area of the lead electrode increased progressively with cycling as a result of formation of spongy lead during the negative half-cycle [10,14,15]. Therefore, the prerequisite condition for the formation of intermediate oxides Pb_2O_3, Pb_3O_4 or PbO_n (peak A_2^-) during the subsequent anodic sweep may be the transformation of the electrode surface to a spongy state. Also, this shows that the formation of PbO_2 from PbO is via the formation of intermediate oxides.

After peak A_3, the current density rises again to give the third major anodic peak, A_4. The latter peak had been previously observed in sulfate solutions and had been attributed to the oxidation of $PbSO_4$ to PbO_2 which formed first on the electrode surface according to the following reaction [10,17]:

$$PbSO_4 + 2H_2O = PbO_2 + SO_4^{2-} + 4H^+ + 2e \quad (5)$$

Finally, the sudden increase in the current density is due to oxygen evolution.

The cathodic portion of the CVs in Fig. 4 shows four peaks (C_1, C_2, C_3 and C_4). Peak C_1 is the first cathodic peak, which appears after reversing the direction of potential scan. The peak corresponds to the reduction of the products formed in peak A_4. This is because when the direction of the potential scan reversed before peak A_4 was reached, peak C_1 did not appear (as seen latter). This peak appeared as a composite peak, when the electrode was cycled (sweeps 2 and 3). On the other hand, the peak potential for C_1 occurred, approximately, in the region of the PbO_2/$PbSO_4$ potential and hence it would correspond to the reduction of β-PbO_2 to $PbSO_4$ and α-PbO_2 to $PbSO_4$ [24]. Further reduction of PbO_2 to $PbSO_4$ is inhibited, because the slow diffusion of SO_4^{2-} group into the $PbSO_4$ layer [10,20,21] is very slow. The current density then decreases to a level where unreduced PbO_2, beneath the $PbSO_4$ layer, will be reduced at peak C_2 to give PbO. This could be explained on the basis that PbO_2 would be reduced first to Pb_3O_4 and the latter to PbO according to the following reactions [10,11,14,20]:

$$3PbO_2 + 2H_2O + 4e = Pb_3O_4 + 4OH^- \quad (6)$$

$$5Pb_3O_4 + 11H_2O + 10e = 3[5PbO \cdot 2H_2O] + 10OH^- \quad (7)$$

Once the above process is completed, the current density falls until the cathodic peak C_3 is reached. Within this peak potential, the inner layer of PbO which formed during the reduction of PbO_2 and the outer $PbSO_4$ layer would be reduced simultaneously to give spongy lead (see below). Similar conclusions were reached recently [10], on the basis of data obtained from the galvanostatic oxidation of Pb in Na_2SO_4 solution. On the other hand, Pavlov and Iordanov [25] and Valeriote and Gallop [26] have pointed out that the H^+ and OH^- ions can diffuse and migrate through the $PbSO_4$ layer. So in the reduction process of the PbO, OH^- ions must diffuse away from the PbO layer to the bulk solution and H^+ ions must diffuse in the opposite direction. Since PbO is stable only under alkaline conditions

[27], the concentration of the OH^- ions is much greater than that of the H^+ ion within the PbO layer. Therefore, the process of PbO reduction will be limited by the diffusion of OH^- ions passing through the $PbSO_4$ layer [25–27]. An interesting feature here is that in the subsequent sweeps 2 and 3, the cathodic peak C_3 is followed by a small plateau C_3^-. The appearance of this plateau may be due to the presence of a certain quantity of $PbSO_4$ remaining unreduced during the main cathodic peak C_3 on the electrode surface [17].

The last reduction peak C_4 that appears immediately before hydrogen evolution was attributed to the formation of lead hydride, PbH_2 [10,11,19]. This peak is followed by hydrogen evolution. The current density associated with hydrogen evolution decreases with cycling. The decrease in the hydrogen current density may be due to the blocking of the electrode by partially reduced oxides [28].

It is worth mentioning here that the reduction of the oxide film takes place at potentials considerably far from their formation values (shifted in the negative direction). This indicates the irreversibility of the process [10,11]. To avoid any complication results from the effect of cycling, the rest of the results are for the first cycle only.

3.2. Effect of the potential scanning range

In order to understand the behavior of the lead electrode, it is necessary to explore the correspondence between the anodic and cathodic peaks. Fig. 5(a) and (b) shows the CVs of the lead electrode in 0.1 M Na_2SO_4 solution at 35 mV s^{-1}. The voltammograms were started from −2.4 V and reversed at various anodic potentials limits ($E_{\lambda a}$). If the lead electrode was polarized anodically to the end of the shoulder A_1^- and before peak A_1 (curve CV_1 in Fig. 5(a)), the subsequent cathodic reduction curve showed one reduction peak C_3. Previous investigators [6–10] reported that this reduction peak is due to the reduction of the $PbSO_4$ surface layer that formed during the positive half-cycle of the voltammogram and this could be represented by the reverse of reaction (1). On the other hand, when the lead electrode was polarized anodically just after the end of peak A_1 (curve CV_2), the cathodic reduction curves showed also only one single reduction peak C_3. The presence of a single reduction peak indicates that both anodically formed species ($PbSO_4$ and PbO) are reduced simultaneously to Pb [10,24]. According to Varela et al. [29], the electro-reduction of the composite $PbSO_4$–PbO layer can be explained on the basis of a complex mechanism which takes into account the contribution of each single species.

When the lead electrode was polarized anodically after peak A_1 in the passive region, curves CV_3 and CV_4 in Fig. 5(a), the following cathodic reduction curve showed the same reduction peak as in curve CV_2. A distinctive feature of curves CV_3 and CV_4 is that, the amount of charge associated with the cathodic reduction peak C_3 increases and the reduction peak C_4 corresponding to the formation of lead hydride starts to appear. The reduction peak C_4 became more pronounced as the previous anodic potential limits, $E_{\lambda a}$, was shifted into a more positive direction (as shown latter in curves CV_5 and CV_6). This may be attributed to the fact that as the anodic potential limit ($E_{\lambda a}$) shifted in a more positive direction, more reactions take place on the electrode surface and, therefore, convert the electrode surface to a spongy state during the cathodic half-cycle.

If the lead electrode was polarized anodically up to the end of peak A_3 and before peak A_4, curve CV_5 in Fig. 5(b), the subsequent cathodic curve appeared the same as was observed in curves CV_3 and CV_4. In addition, the peak C_2 started to appear, corresponding to reduction of PbO_2 to PbO (reactions 6 and 7).

It is worth mentioning here that when the electrode was polarized anodically to a potential +1.750 V or more, curve CV_6 in Fig. 5(b), the subsequent cathodic curve showed the same behavior as discussed above in Fig. 4. Generally from Fig. 5(a) and (b) it was found that, the height of the cathodic current peak and the corresponding peak potential depends on the anodic limit of the potential excursion, $E_{\lambda a}$. Also, the irreversibility of the film formation–reduction reaction, given by the difference between anodic and cathodic peak potential, increases with $E_{\lambda a}$.

Fig. 6 shows the dependence of the anodic (Q_a) and cathodic (Q_c) charges on $E_{\lambda a}$. The quantity of electricity was integrated between −2.000 and +1.750 V versus (SCE) in order to exclude the charge involved in both lead hydride and oxygen evolution at two extremes of the CVs. It should be noted that as the anodic limit of the potential excursion shifted to more positive potentials, both anodic and cathodic charges increased. Furthermore, the ratio of the anodic to cathodic charges, Q_a/Q_c was slightly greater than 1 (Fig. 6). This indicates that part of the anodic charge was used to produce a soluble species [10,11,28]. The anodic soluble reaction produced may be the biplumbite ion $HPbO_2^-$ in a small quantity according to the electrochemical reaction [10,11,14,19]

$$Pb + 3OH^- = HPbO_2^- + H_2O + 2e \quad (8)$$

and/or from PbO through a chemical reaction

$$PbO + OH^- = HPbO_2^- \quad (9)$$

The dissolution of some PbO_2 as the plumbate ions PbO_3^{2-} can be excluded as a plausible explanation [11].

3.3. Effect of sulfate concentration

The CVs of the lead electrode were traced in Na_2SO_4 solutions of various concentrations (0.05–0.5 M) at a sweep rate 35 mV s^{-1}. The scan was carried out between −2.4 and extended to +2.2 V versus SCE. The lead electrode was cathodically maintained at −2400 mV for 10 min in order to reduce any oxides that formed spontaneously on the metal surface before the experiment.

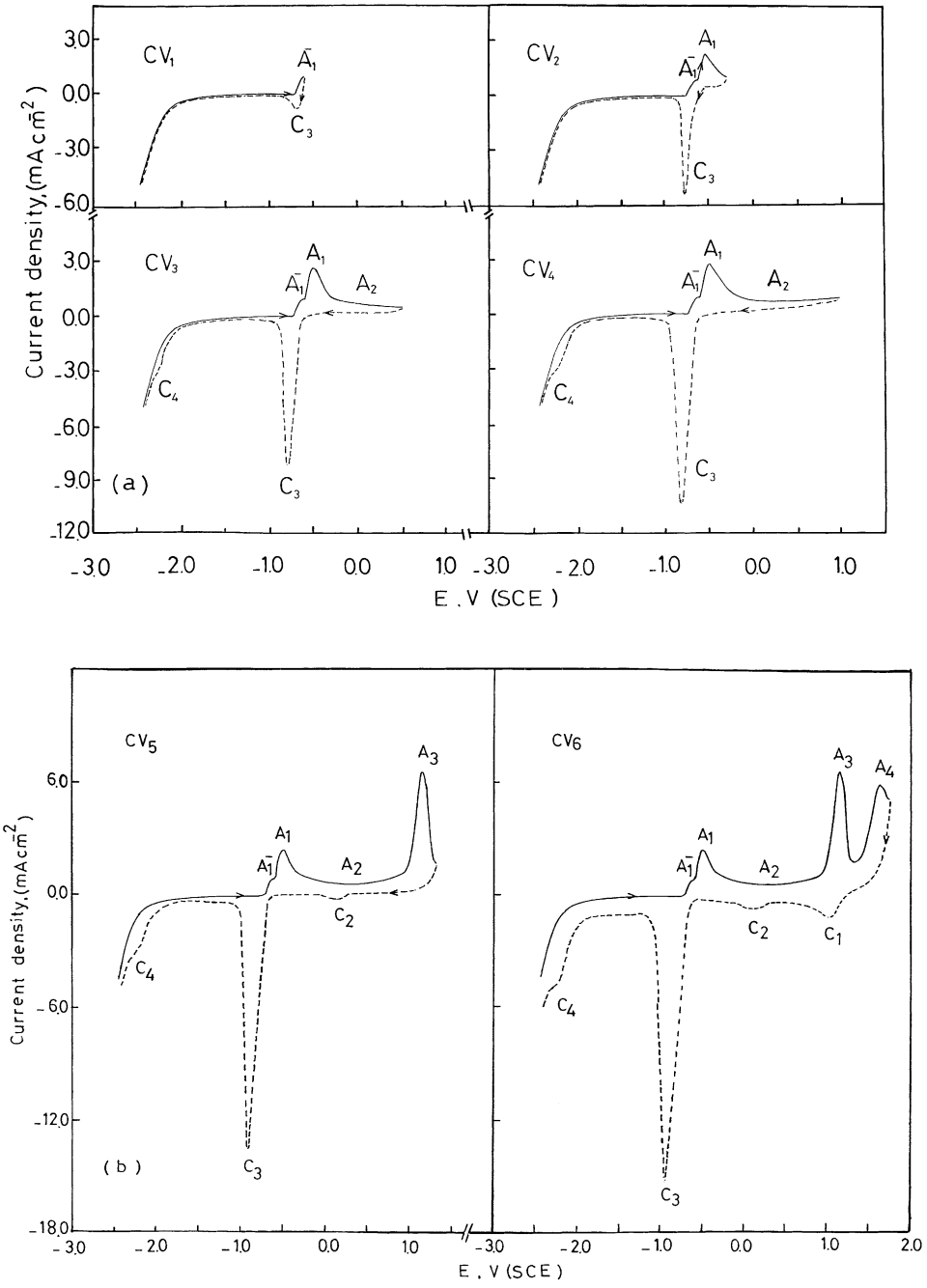

Fig. 5. (a) and (b) Cyclic voltammograms of the lead electrode in 0.1 M Na_2SO_4 solution with the sweep rate 35 mV s^{-1} at selected voltage excursions ($E_{\lambda a}$). The anodic polarization is the solid lines and their reduction curves is dashed lines.

As the sulfate concentration increased, the potential of shoulder A_1^-, peak A_1 and peak A_3 were observed to shift towards more negative values. The relation between the peak potential, E_p and concentration of sulfate anions was linear, obeyed the Nernst equation [30] and could be represented by

$$E_p = E^0 - \frac{0.059}{n} \log a_{SO_4^{2-}} \quad (10)$$

where E_p, E^0, n and a are the measured potential of shoulder or peak, the standard potential, the number of electrons involved in the reaction and the activity of Na_2SO_4 solutions, respectively. Under such conditions, a plot of E_p versus $\log a_{SO_4^{2-}}$ is a straight line with slopes of 59 and 30 mV for one- and two-electron transfer reactions, respectively.

Fig. 7 shows plots of E_p versus $\log C_{SO_4^{2-}}$ for shoulder A_1^-, peak A_1 and speak A_3. Three straight lines were obtained having slopes of 30, 30 and 40 mV per decade for shoulder A_1^-, peak A_1 and peak A_3, respectively. The slope obtained for shoulder A_1^- equals 30 mV per decade,

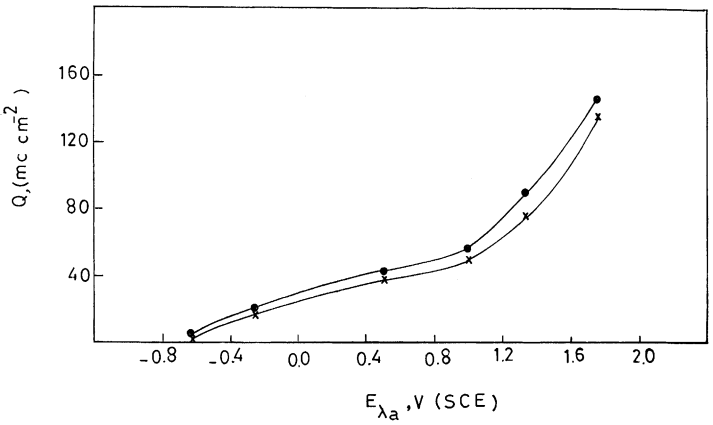

Fig. 6. Dependence of the anodic, Q_a (●), and the cathodic, Q_c (×) charges on $E_{\lambda a}$. Calculated from Fig. 5(a) and (b).

which gave a value of 2 for the number of electrons involved in the electrode reaction process. This indicated that reaction (1) occurred during the formation of shoulder A_1^-.

Also, the value of 30 mV per decade for the slope corresponding to peak A_1, Fig. 7, is an indication that the current density of this peak is supported by a two-electron transfer reaction whose overall reaction likely to be [6–10].

$$Pb + 2OH^- = PbO + H_2O + 2e \quad (11)$$

The value of 40 mV per decade for the slope corresponding to peak A_3, Fig. 7, is somewhat larger than the theoretical value of 30 mV per decade for a two-electron transfer reaction [31]. Such a value obtained might be explained in terms of a two-electron transfer reaction (Eq. (12)) and possibly a small proportion of a one-electron transfer reaction owing to the formation of a non-stoichiometric lead oxide (PbO_{1+n}, $n = 0.57$) [32]. Thus, peak A_3 may result from the following overall reaction [11,33]:

$$PbO + 2OH^- = PbO_2 + H_2O + 2e \quad (12)$$

The dependence of the current-densities of shoulder A_1^-, peak A_1 and peak A_3 on the concentration of Na_2SO_4 is of a particular interest. A plot of the two variables on a double logarithmic scale is shown by the curves in Fig. 8. It is clear

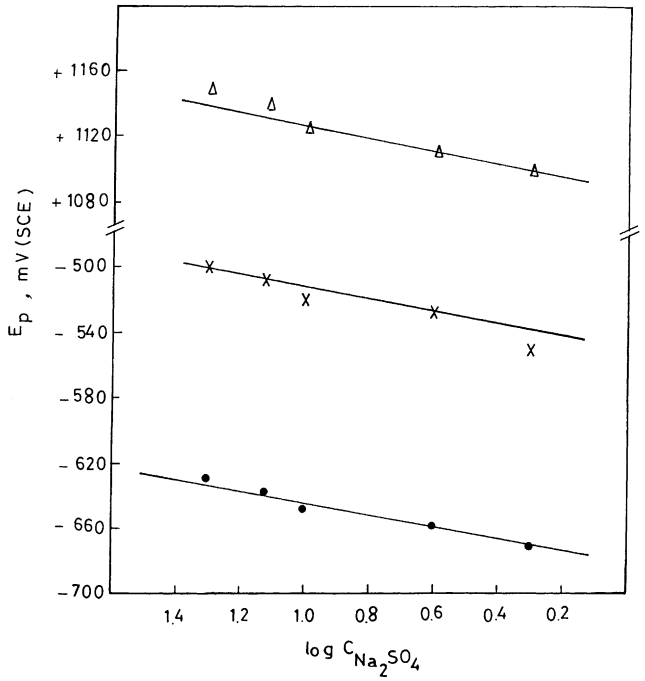

Fig. 7. Relation between the peak potential, E_p, and $\log C_{Na_2SO_4}$ for shoulder A_1^- (●); peak A_1 (×) and peak A_3 (△).

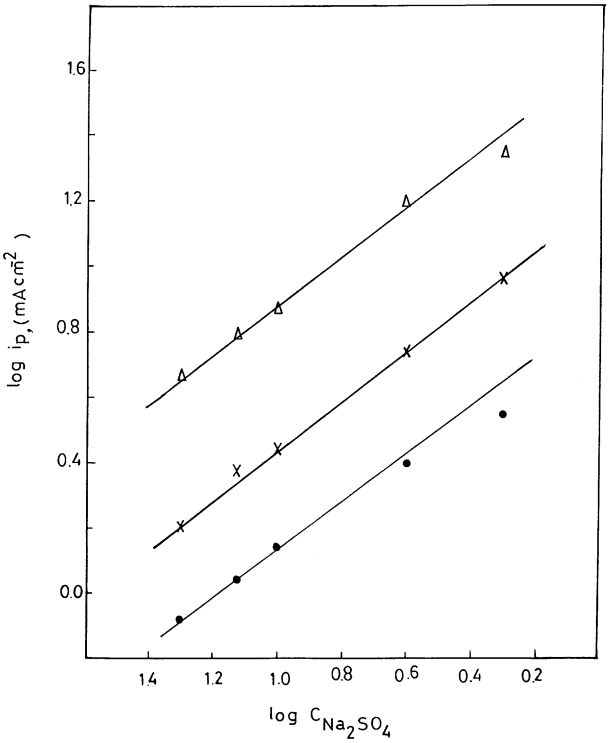

Fig. 8. Variation of $\log i_p$ with $\log C_{Na_2SO_4}$ for shoulder A_1^- (●); peak A_1 (×) and peak A_3 (△).

that the data are well represented by three parallel lines, within the concentration range studied, according to

$$\log i_p = a + b \log C_{SO_4^{2-}} \quad (13)$$

where a and b are constants. The value of b is about 0.75, well within the expected value (1.0) for a diffusion process [33].

3.4. Effect of voltage scanning rate

Fig. 9(a) and (b) shows the CVs recorded for the lead electrode in 0.1 M Na_2SO_4 solution at various sweep rates, $v = dE/dt$, ranging between 25 and 125 mV s^{-1}. In all experiments, the scan of the anodic potential was started at −2400 and extended to +2200 mV. The figure reveals that an increase in the sweep rate, led to a marked increase in the current flowing along the whole range of the CVs as well as the potential of both anodic and cathodic peaks. For an irreversible system, the theoretical equation of i_p at 25°C is given by [34]

$$i_p = 2.99 \times 10^5 n(\alpha n)^{0.5} ACD^{0.5} v^{0.5} \quad (14)$$

where A, D, C, v and n are the surface area of the reaction, the diffusion coefficient, the concentration of the reaction species, the potential sweep rate, and the electron number of the reaction of the rate-controlled step, respectively.

The effect of sweep rate on the current density along shoulder peak A_1^-, peak A_2 and peak A_3 is shown in Fig. 10. The relation between $i_{A_1^-}$ for the shoulder and $v^{0.5}$ gives a straight line extrapolated to the origin. This indicates that the formation of $PbSO_4$ is controlled by diffusion of the SO_4^{2-} anion to the anode surface. This conclusion is in a good agreement with our previous results under galvanostatic polarization study [10].

With regard to peak A_1, a linear relationship between i_{A_1} and $v^{0.5}$ is observed with a small intercept in Fig. 10. In this connection it has been suggested that the presence of an intercept indicates that the rate-determining step in the formation of PbO is not a single diffusion-controlled process [11]. Such processes might be diffusion of soluble species from the reaction between PbO and hydroxide away from the electrode whereas the hydroxide ions present in the electrolyte diffuse towards the electrode–solution interface.

Also, as can be seen in Fig. 10, a linear proportionality passing through the origin is obtained between i_{A_3} and $v^{0.5}$. This observation suggests the occurrence of anther diffusion-controlled process during the formation of PbO_2. The latter process may be correlated with the diffusion of some PbO_2 as a soluble species, PbO_3^{2-} away from the electrode surface [11].

A distinctive feature of Fig. 9(a) and (b) is that, as the sweep rate increases, the anodic peaks are shifted towards more positive values of potential, whereas the cathodic peaks are shifted in the negative direction. It has been established that with the greater separation between anodic

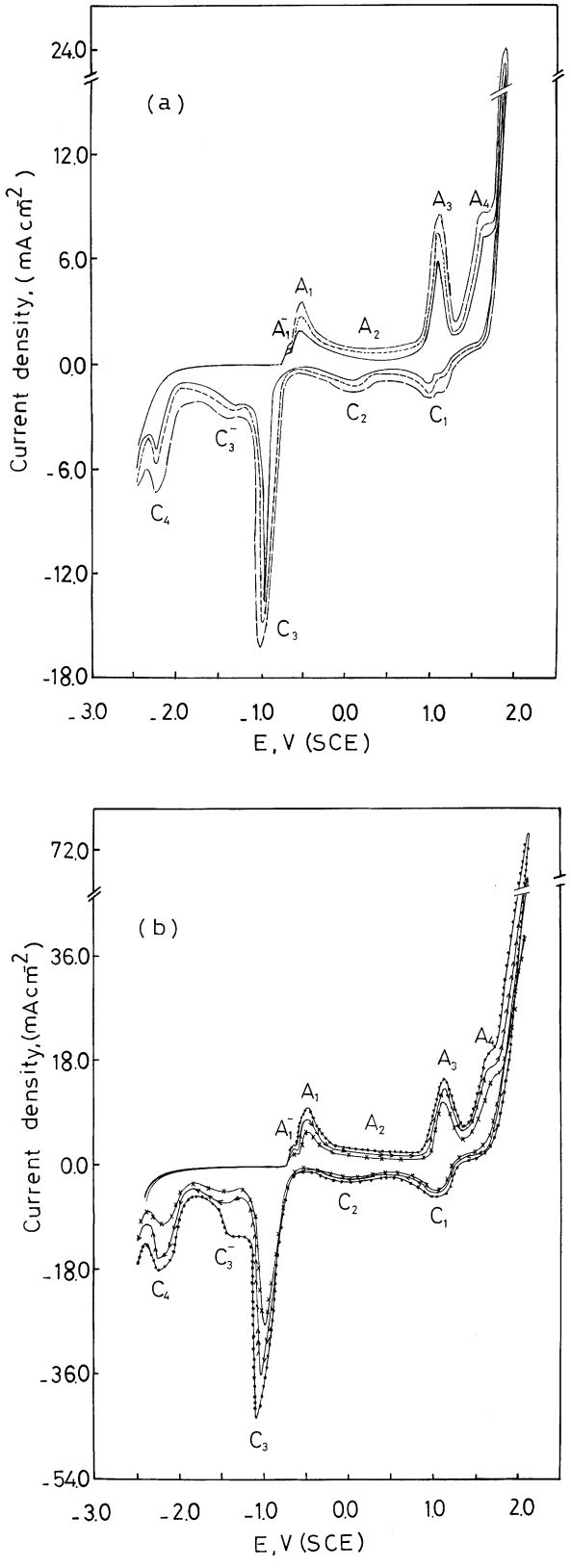

Fig. 9. (a) and (b) Effect of voltage scanning rates on CVs of lead in 0.1 M Na_2SO_4 solution, (a) (—) 25 mV s^{-1}; (- - -) 35 mV s^{-1}; (– – –) 45 mV s^{-1}. (b) (×) 75 mV s^{-1}; (>) 100 mV s^{-1}; (●) 125 mV s^{-1}.

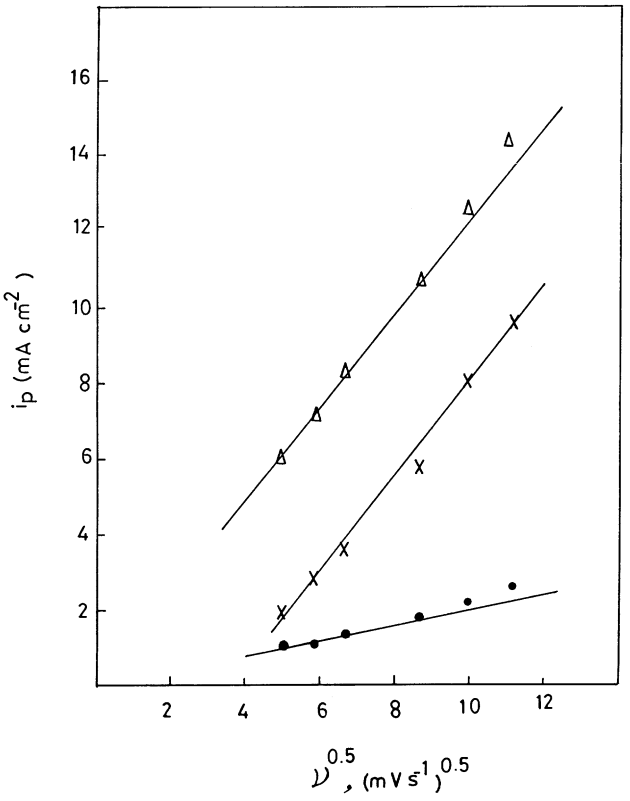

Fig. 10. Dependence of current density, i_p, along shoulder A_1^- (●); peak A_1 (×) and peak A_3 (△) on the square root of sweep rate in 0.1 M Na_2SO_4.

and cathodic peaks, are likely to indicate the irreversible formation of a passive film on the electrode surface [10,11].

4. Conclusions

The CVs of lead in Na_2SO_4 solutions show the following:

1. The initial state of the electrode surface is an important factor, which affects the shape of the voltammograms.
2. The anodic portions of the CVs are characterized by the formation of $PbSO_4$, PbO, intermediate oxides, PbO_2 and transformation of $PbSO_4$ to PbO_2 on the electrode surface, respectively, before oxygen evolution.
3. The cathodic portions show the reduction of PbO_2 to $PbSO_4$, PbO_2 to PbO and the latter with $PbSO_4$ to spongy lead, respectively, followed by the formation of PbH_2 before hydrogen evolution.
4. As the concentration of sulfate anion increases, the anodic oxidation peaks corresponding to $PbSO_4$, PbO and PbO_2 are shifted towards more active values.
5. Also, the current density flowing along the anodic oxidation peaks corresponding to $PbSO_4$, PbO and PbO_2 varies with the concentration of the electrolyte according to: $\log i_p = a + b \log a_{SO_4^{2-}}$.
6. An increase in the sweep rate led to a marked increase in the current flowing along the whole range of the CVs as well as the potential of both anodic and cathodic peaks. This is thought to be 'due to the formation of a passive film on the electrode surface.

References

[1] J.L. Dawson, in: A.T. Kuhn (Ed.), Electrochemistry of Lead, Academic Press, London, 1979, p. 309.
[2] K.R. Bullock, J. Electroanal. Chem. 222 (1987) 347.
[3] P. Veluchamy, M. Shimizu, H. Minoura, J. Electroanal. Chem. 379 (1994) 253.
[4] W. Hoffman, Lead and Lead Alloys, 2nd Edition, Springer, New York, 1970.
[5] J. Boulton, Atomic Energy of Canada Ltd., Report AECL-6314, 1978.
[6] A.A. Abdul Azim, M.M. Anwar, Corros. Sci. 9 (1969) 245.
[7] A.A. Abdul Azim, V.K. Gouda, L.A. Shalaby, S.E. Afifi, Br. Corros. J. 8 (1973) 76.
[8] V.K. Gouda, L.A. Shalaby, A.A. Abdul Azim, Br. Corros. J. 8 (1973) 83.
[9] R.J. Thibeau, C.W. Brown, A.Z. Goldfarb, R.H. Heidersbach, J. Electrochem. Soc. 127 (1980) 1913.
[10] E.E. Abd El Aal, J. Power Sources 75 (1998) 36.
[11] E.E. Abd El Aal, S. Abd El Wanees, A. Abd El Aal, J. Mater. Sci. 28 (1993) 2607.
[12] D. Geana, A.A. El Miligy, W.J. Lorenz, J. Appl. Electrochem. 4 (1974) 337.
[13] S.M. Abd El Haleem, A.A. Abd El Aal, Corros. Prevent. Cont. 29 (1982) 13.
[14] E.E. Abd El Aal, Bull. Soc. Chem. Fr. 128 (1991) 351.
[15] A.M. Abd El Halim, M.H. Fawzy, A. Saty, J. Chem. Technol. Biotechnol. 58 (1993) 165.
[16] F.M. Abd El Wahab, M.G.A. Khedr, H.A. El Shayeb, J. Mater. Sci. 17 (1982) 3401.
[17] S.S. Abd El Rehim, A.M. Abd El Halim, E.E. Foad, Surf. Technol. 21 (1984) 161.
[18] E.E. Abd El Aal, Anti. Corros. Meth. Mater. 46 (1999) 349.
[19] M. Pourbaix, Atlas of Electrochemical Equilibria, Pergamon Press, Oxford, UK, 1966, p. 486.
[20] D. Pavlov, R. Popova, Electrochim. Acta 15 (1970) 1483.
[21] P. Ruetschi, J. Electrochem. Soc. 120 (1973) 331.
[22] E.E. Abd El Aal, Corros. NACE 48 (1992) 282.
[23] V.I. Birss, M.T. Shevalier, J. Electrochem. Soc. 137 (1990) 2643.
[24] Y. Yamamoto, K. Fumino, T. Ueda, M. Nambu, Electrochim. Acta 37 (1992) 199.
[25] D. Pavlov, N. Iordanov, J. Electrochem. Soc. 117 (1970) 1103.
[26] E.M.L. Valeriote, L.D. Gallop, J. Electrochem. Soc. 124 (1977) 370.
[27] Y. Guo, Electrochim. Acta 37 (1992) 495.
[28] S.D. Kapusta, N. Hacherman, Electrochim. Acta 25 (1980) 1625.
[29] F.E. Varela, L.M. Gassa, J.R. Vilche, Electrochim. Acta 37 (1992) 1119.
[30] A.J. Bard, L.R. Faulkner, Electrochemical Methods-Fundamental and Applications, Wiley, New York, 1980, p. 91.
[31] S.M. Abd El Haleem, B.G. Ateya, J. Electroanal. Chem. 117 (1981) 309.
[32] J.S. Buchanan, N.P. Freestone, L.M. Peter, J. Electroanal. Chem. 128 (1985) 383.
[33] P. Delehay, New Instrumental Methods in Electrochemistry, Interscience, New York, 1954 (Chapter 6).
[34] H.R. Thirsk, J.A. Harrison, A Guide to the Study of Electrode Kinetics, Academic Press, London, 1972, p. 61.